ELSEVIER

Journal of Alloys and Compounds 434–435 (2007) 650–654

Journal of ALLOYS AND COMPOUNDS

www.elsevier.com/locate/jallcom

The thermal stability of maghemite-silica nanocomposites: An investigation using X-ray diffraction and Raman spectroscopy

P.P.C. Sartoratto [a], K.L. Caiado [a], R.C. Pedroza [b], S.W. da Silva [b], P.C. Morais [b,*]

[a] *Universidade Federal de Goiás, Instituto de Química, 74001-970 Goiânia-GO, Brazil*
[b] *Universidade de Brasília, Instituto de Física, Núcleo de Física Aplicada, 70919-970 Brasília-DF, Brazil*

Available online 28 September 2006

Abstract

Maghemite-silica nanocomposites consisting of 5 nm magnetic nanoparticles dispersed in silica xerogel were prepared by the sol–gel technique. The thermal stability of samples with 0.013 and 0.200 Fe/Si molar ratio was investigated in the temperature range of 120–1400 °C by X-ray, FTIR and Micro-Raman spectroscopy. Depending on the nanoparticle content, the silica matrix provides extra stabilization of γ-Fe_2O_3 nanoparticles against transformation into α-Fe_2O_3 and ε-Fe_2O_3. In nanocomposite samples presenting low nanoparticle concentration, γ-Fe_2O_3 was the only iron oxide phase found up to 900 °C. However, above 900 °C, ε-Fe_2O_3 was the dominant phase. For high nanoparticle contents, mixtures of α-Fe_2O_3 and γ-Fe_2O_3 phases were identified at 500 and 700 °C, though α-Fe_2O_3 and ε-Fe_2O_3 phases were found at higher temperatures.

Keywords: Nanocomposites; Sol–gel synthesis; X-ray diffraction; Micro-Raman spectroscopy; FTIR

1. Introduction

Nanocomposites are material systems containing one or more nanocrystalline component dispersed in a polymer, glass or ceramic template [1–3]. These systems exhibit many unique functional properties with valuable technological applications. Among them, transparent magnetic nanocomposites are promising materials for applications in magneto-optical, recording media, displays and device such as waveguides, isolators, modulators and switches [4,5]. The magnetic behavior and the optical properties of magnetic nanocomposites are strongly affected by the characteristics of both the embedded magnetic nanophase and the host template. Nanocomposites containing maghemite (γ-Fe_2O_3) nanoparticles dispersed in silica have been synthesized by mechanical activation [6], by heating a mixture of iron nitrate and silicon alkoxide between 700 and 900 °C [7], or by incorporating previously synthesized nanoparticles dispersed in aqueous medium and latter on added to the template by the sol–gel method [3]. Preparation of pure γ-Fe_2O_3 nanophase presents some difficulties arising from the different metal oxidation states, which can lead to the presence of various oxides (FeO, Fe_2O_3 and Fe_3O_4). Besides that, there are a number of polymorphs of the iron (III) oxide system, such as α-Fe_2O_3, ε-Fe_2O_3, β-Fe_2O_3 and amorphous Fe_2O_3 [8,9]. Hematite is the most thermodynamically stable phase; at temperatures around 380 °C γ-Fe_2O_3 nanoparticles aggregate and are transformed into α-Fe_2O_3. Attempts have been made to stabilize nanometric γ-Fe_2O_3 particles in SiO_2 matrix [10,11]. The method of incorporating previously synthesized nanoparticles into an alkoxide sol–gel mixture seems to be the best option since it guarantees that a single magnetic phase and narrow-sized nanoparticles are uniformly distributed in the silica xerogel template [12]. However, sol–gel processing with the aim of preparing monolithic glasses for optical applications requires thermal treatment for the drying and densification steps that may cause iron oxide to change phase. It has been shown that silica matrix acts as antisintering agent, which stabilizes maghemite particles up to 1000 °C against thermal transformation into hematite [3]. Above this temperature, mixtures of ε-Fe_2O_3 and α-Fe_2O_3 phases can be obtained [10]. It must be pointed out that it is very difficult to obtain the pure ε-Fe_2O_3 phase, but the management of the sol–gel processing with the aim of controlling the confinement of nanoparticles inside the pores of a silica xerogel is an opportunity to optimize the synthesis of this rare polymorph [13,14]. In this study, X-ray diffraction, FTIR and Micro-Raman spectroscopy were used to investigate the thermal stability of maghemite-silica

* Corresponding author. Tel.: +55 61 3273 6655; fax: +55 61 3272 3151.
E-mail address: pcmor@unb.br (P.C. Morais).

0925-8388/$ – see front matter © 2006 Elsevier B.V. All rights reserved.
doi:10.1016/j.jallcom.2006.08.208

nanocomposites and characterize the iron oxide phases in low and high nanoparticle containing samples.

2. Experimental procedures

The nanocomposite samples were prepared using the sol–gel procedure. A previously synthesized aqueous-based maghemite magnetic fluid (MF) sample was dispersed in tetraethoxysilane/ethanol/H_2O/H^+ sol–gel system, in the 1:4:12:0.005 molar ratio. A typical sol–gel precursor mixture contained 10 mL tetraethoxysilane (TEOS), 10 mL ethanol, 10 mL water and 100 μL of 0.50 mol/L perchloric acid. The sol–gel precursor mixture was stirred for 1 h, before mixing with 2 or 30 mL of the aqueous-based maghemite MF sample, producing two composite samples labelled LW and HG, respectively. After adding the MF sample, the mixture was stirred for extra 30 min, poured into polystyrene recipients and left to slowly gelate and dry at room temperature for 30 days. After this period of time, all samples were powdered and then heated in air at different temperatures, in the range of 120–1400 °C for 1 h.

Maghemite nanoparticles were obtained by bubbling oxygen in an acid (pH 3.5) aqueous suspension containing magnetite nanoparticles, at 90 °C for 9 h. Magnetite was synthesized by chemical co-precipitation of Fe (II) and Fe (III) ions in alkaline medium, following a procedure described in literature [15]. The aqueous-based maghemite MF was prepared by peptizing maghemite nanoparticles in a 0.5 mol L^{-1} $HClO_4$ aqueous solution. The Fe (III)/Fe (II) = 42 molar ratio in the maghemite sample was obtained from the quantitative analysis of iron ions using the *o*-phenantroline colorimetric method. The total concentration of iron in the maghemite MF sample was 2.94×10^{-4} mol L^{-1}, as determined from atomic absorption analysis. The Fe/Si molar ratio in end composite samples (heated at 120 °C until weight was constant) was calculated using atomic absorption data of iron content, considering that all silicon was present as SiO_2. The Fe/Si molar ratio in the two composite samples was estimated to be 0.013 and 0.200. Both composite samples contained residual perchlorate and sodium ions coming from the maghemite MF sample. The original maghemite powder sample was also heated in the range of 120–1400 °C, for 1 h in air.

Powder X-ray diffraction of both maghemite and composite samples were recorded in a Schimadzu XRD 6000 equipment, using the Cu Kα radiation. The X-ray line broadening of the most intense diffraction peak (3 1 1) of the stock maghemite powder sample provided the average diameter (5 nm) of the nanocrystalline domain. The average nanoparticle size was estimated using the Scherrer's equation [16,17]. The diffuse reflectance spectra of both maghemite and composite samples were obtained in a FTIR Bomem, MB 100 equipment, with samples dispersed in KBr (1%). The Raman system used to record the spectra was a commercial triple spectrometer (Jobin–Yvon Model T64000) equipped with a CCD detector. The 514 nm line from an Argon ion laser was used to illuminate the samples. All measurements were performed at room temperature.

3. Results and discussion

The synthetic method used for preparation of maghemite nanoparticles produced a sample still containing around 2% of Fe (II) ions. Despite the prolonged time of the procedure step used for magnetite oxidation (bubbling oxygen for 9 h), magnetite was not fully oxidized to maghemite, probably due to oxygen diffusion limitation. The powder X-ray diffraction patterns of the sample heated at various temperatures are shown in Fig. 1. Note that the typical X-ray peaks of the maghemite spinel structure (2 2 0, 3 3 1, 4 0 0, 4 2 2, 5 1 1, 4 4 0) are observed in the diffractograms of the non-heated and heated (300 and 500 °C) maghemite samples (JCPDF 25-1402). The lattice parameter for the cubic arrangement was calculated to be 0.837 nm, which is an intermediate value between those for bulk maghemite (0.839 nm) and bulk magnetite (0.834 nm). The lattice parameter of the synthesized maghemite samples may vary due to a number of facts, including stoichiometry shift, nanocrystalline size and

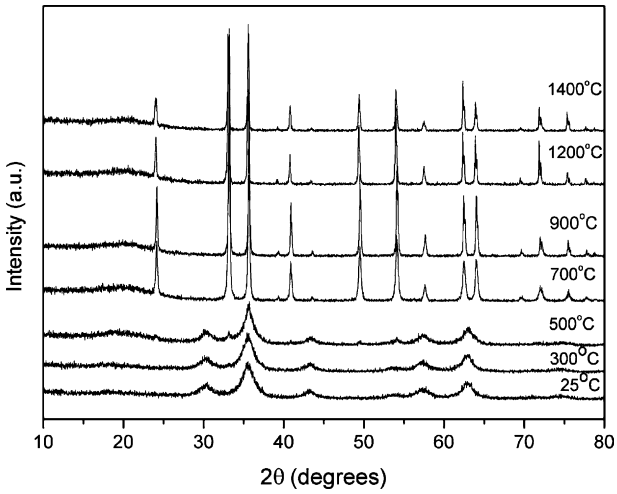

Fig. 1. X-ray diffractograms of the maghemite powder sample heated in the temperature range of 300–1400 °C.

ordering of octahedral and tetrahedral vacant sites [18]. Thus, the sample prepared in this study may be considered as γ-Fe_2O_3 doped with a small amount of Fe (II) ions, which will be labelled maghemite for simplicity purposes. The synthesized maghemite powder sample was stable upon heating up to 300 °C. However, the 500 °C heated maghemite powder sample showed the X-ray peaks (0 1 2, 1 0 4, 1 1 0, 1 1 3, 0 2 4, 1 1 6, 0 1 8, 2 1 4, 3 0 0, 1 0 1, 2 2 0) typical of the rhomboedric structure (JCPDF 87-1165) of hematite. The diffractograms of the maghemite powder sample heated in the temperature range of 700–1400 °C shows only the hematite phase.

The X-ray diffractograms of the LW and HG composite samples, respectively characterized by the Fe/Si = 0.013 and Fe/Si = 0.200 molar ratios, are shown in Fig. 2. In the case of the LW composite sample the maghemite phase is stable upon heating up to 900 °C, although the maghemite X-ray peaks cannot be observed due to the strong background provided by the amorphous silica matrix. Upon heating in the range of 1200–1400 °C the LW composite sample shows the X-ray pattern of cristobalite (JCPDF 77-1317), though minor peaks can also be observed, but not matching those of the γ-Fe_2O_3 or α-Fe_2O_3 phases. Instead, the minor peaks can be attributed to the ε-Fe_2O_3 phase (JCPDF 16-0653). The HG composite sample, however, shows a different behaviour upon heating; the maghemite phase being stable only up to 300 °C. Both maghemite and hematite phases were observed in the X-ray diffractogram of the HG composite sample heated at 500 °C. We observed that the HG composite sample and the synthesized maghemite sample reveal similar behaviour as far as the thermal treatment is concerned. However, thermal treatment of the HG composite sample at 900, 1200 and 1400 °C resulted in the onset of both the ε-Fe_2O_3 phase and the cristobalite phase, though a small amount of α-Fe_2O_3 was also observed. Concerning the stability of the maghemite nanoparticles, the iron oxide phase produced upon heating and the crystallinity of the silica matrix, the thermal behaviour of the HG and LW composite samples is quite different.

Fig. 3 shows the FTIR spectra (in the 400–1500 cm^{-1} range) of the LW and HG composite samples submitted to different

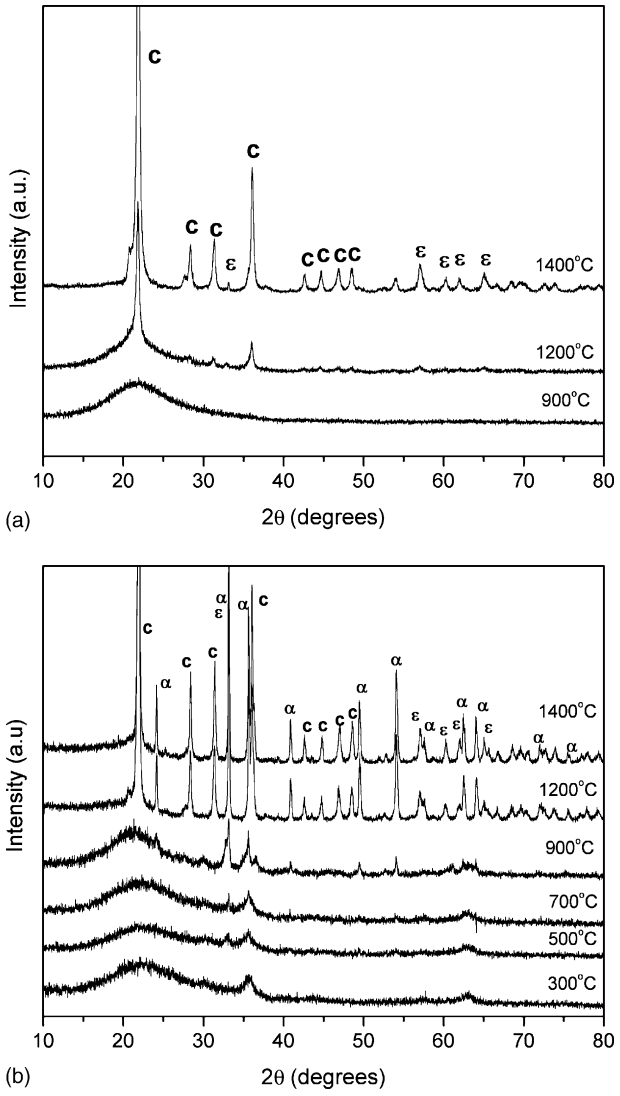

Fig. 2. X-ray diffractograms of: (a) LW nanocomposite sample (Fe/Si = 0.013) heated at 900, 1200 and 1400 °C and (b) HG nanocomposite (Fe/Si = 0.200) heated in the temperature range of 300–1400 °C.

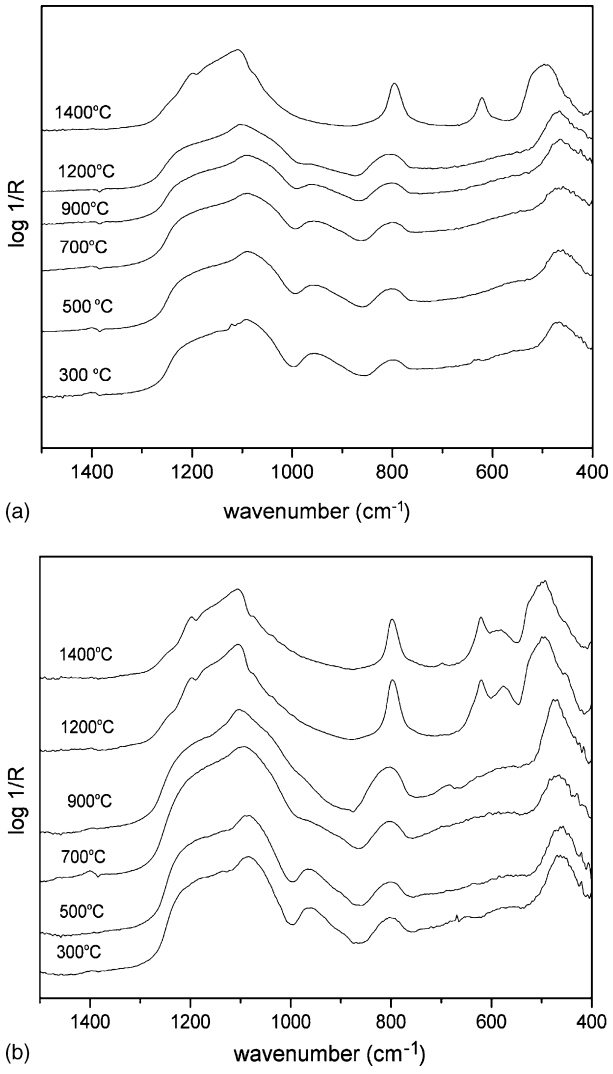

Fig. 3. FTIR spectra of: (a) LW nanocomposite sample (Fe/Si = 0.013) and (b) HG nanocomposite (Fe/Si = 0.200) heated in the temperature range of 300–1400 °C.

thermal treatments. All spectra show the superimposed asymmetric Si–O–Si stretching bands at 1100 and 1200 cm^{-1} plus the symmetric Si–O–Si stretching band around 800 cm^{-1}. The shape and width of the stretching bands change depending upon the sample's thermal treatment, according to the degree of crystallinity of the silica matrix. For the 1200 °C thermal treatment, the short distance ordering of the silica array is greater in the HG than in the LW composite sample. The Si–O stretching band of Si–OH groups peaking at 970 cm^{-1} loses intensity as the sample is heated. This is more pronounced in the HG than in the LW composite sample. As the composite samples are heated the silanol groups of the amorphous silica condensate to form siloxane bonds and may disappear when silica is fully crystallized into cristobalite. Besides that, the condensation reaction can be favored when the mobility of silica arrays is enhanced. This must be the case of the HG composite sample that contains a higher amount of sodium ions, thus lowering the transition vitreous temperature. The FTIR spectra in the 400–800 cm^{-1} region also reveal interesting aspects. Upon heating at 1400 °C the LW composite sample shows a new band peaking at 620 cm^{-1}. However, the HG composite sample heated at 1200 °C revels two new bands at 620 and 570 cm^{-1}. The 620 and 570 cm^{-1} bands are attributed to the Fe–O stretching modes of the ε-Fe_2O_3 and α-Fe_2O_3 phases, respectively. Therefore, the FTIR data is in excellent agreement with the X-ray observations regarding the ε-Fe_2O_3 as the main iron oxide phase in the LW composite sample whereas both ε-Fe_2O_3 and α-Fe_2O_3 phases were found in the HG composite sample.

The Raman spectra of LW and HG composite samples, in the low wavenumber region, are shown in Fig. 4. The Raman spectra of the LW composite sample heated up to 900 °C is dominated by the 490 cm^{-1} band, attributed to the O_3SiOH stretching modes of the silica matrix defects [19]. However, broad Raman bands around 360 and 700 cm^{-1}, attributed to the Fe–O stretching modes of the maghemite phase are also present [20]. Other main Raman bands appear at 240, 310 and 428 cm^{-1} when the LW composite sample is heated at 1200 °C, whose

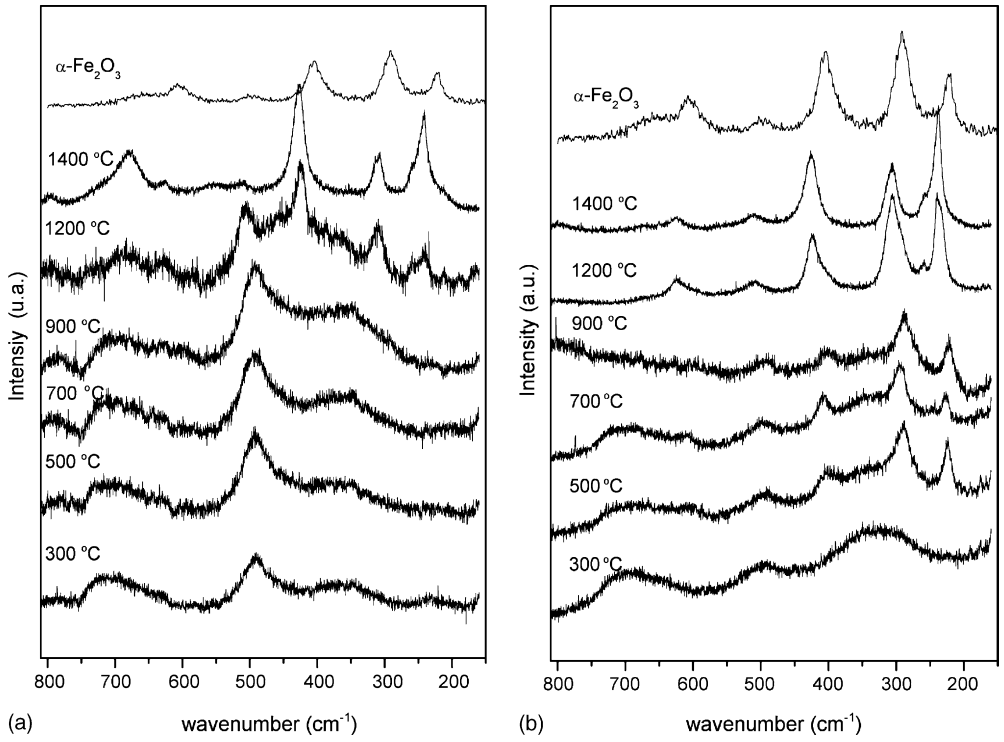

Fig. 4. Raman spectra of: (a) LW nanocomposite sample (Fe/Si = 0.013) and (b) HG nanocomposite (Fe/Si = 0.200), heated in the temperature range of 300–1400 °C. The hematite spectra is also included.

profiles dominate the spectra when sample is further heated at 1400 °C. It is worthwhile to note that the position and relative intensities of these bands do not match those observed in the hematite Raman spectra, as can be seen in Fig. 4 for comparison. Thus, the set of the three Raman bands, peaking at 240, 310 and 428 cm^{-1}, may be attributed to the Fe–O stretching modes of the ε-Fe_2O_3 phase. The weak band around 680 cm^{-1} is the symmetric stretching mode of SiOSi groups of the crystallized silica [21]. The Raman spectra of the HG composite sample heated up to 300 °C are dominated by the Fe–O stretching modes of the maghemite phase, peaking at 360, 502 and 700 cm^{-1} [20]. When the HG composite sample is heated at 500 and 700 °C, the maghemite Raman bands are still present but the hematite Raman bands at 221, 290 and 405 cm^{-1} also appear [22]. Upon heating at 1200 and 1400 °C, this set of Raman bands shift to higher wavenumbers, meaning that the bands of the ε-Fe_2O_3 phase dominate the Raman spectra although the hematite phase may be also present, as observed by X-ray diffraction and FTIR measurements.

These results are somewhat similar to those reported by Chanéac et al. [23], though no α-Fe_2O_3 phase was observed in the LW composite sample using X-rays diffraction, FTIR and Raman measurements. Besides, we have observed that the presence of sodium ions in the composite samples changes the temperature the α-Fe_2O_3 phase begins to crystallize. We have prepared a HG composite sample incorporating the maghemite MF sample free of sodium ions and observed that the α-Fe_2O_3 begins to crystallize only at 900 °C. Our findings indicate that grains of both α-Fe_2O_3 and ε-Fe_2O_3 phases are formed only if the agglomeration of γ-Fe_2O_3 nucleus is efficient to produce enough amount of iron oxide to rearrange into the new crystalline structures [10]. Which iron oxide phase will be formed within the silica matrix depends upon two factors: (i) the temperature the matrix begins to soften to permit efficient mass transport and (ii) the amount of maghemite nanoparticles which determines whether the grains are limited or not to grow up. Actually, samples with both high sodium and nanoparticle content may not stabilize the maghemite phase, resulting in mixtures of α-Fe_2O_3 and ε-Fe_2O_3 phases when heated at temperatures above 300 °C. Samples with both very low sodium and nanoparticle content may stabilize the maghemite phase upon heating up to 900 °C and may result in ε-Fe_2O_3 as the dominant phase when heated at higher temperatures. This last point is supported by the fact that formation of the ε-Fe_2O_3 phase may require agglomeration of a smaller number of maghemite grains than formation of α-Fe_2O_3 phase [24].

4. Conclusion

Maghemite nanoparticles were successfully incorporated into a silica xerogel template while the thermal stability of the maghemite phase was evaluated. Nanocomposites with both high sodium and nanoparticle content may not stabilize the maghemite phase, resulting in mixtures of α-Fe_2O_3 and ε-Fe_2O_3 phases when heated at temperatures above 300 °C. Samples with both very low sodium and nanoparticle content may stabilize the maghemite phase upon heating up to 900 °C and may present mainly ε-Fe_2O_3 when heated at higher temperatures. Micro-Raman spectroscopy was shown to be a quite useful technique to analyse maghemite phase transformations, particularly for very

low nanoparticle containing samples for which X-ray diffraction provides poor information.

Acknowledgments

This work was partially supported by the Brazilian agencies FINATEC and CNPq.

References

[1] R.F. Ziolo, E.P. Giannelis, G.A. Weinstein, M.P. Ohoro, B.N. Ganguly, V. Mehrotra, M.W. Russel, D.R. Huffman, Science 257 (1992) 219–223.
[2] S. Chakrabarti, D. Das, D. Ganguli, S. Chaudhuri, Thin Solid Films 441 (2003) 228–237.
[3] C. Chanéac, E. Tronc, J.P. Jolivet, J. Mater. Chem. 6 (1996) 1905–1911.
[4] M. Sugimoto, J. Am. Ceram. Soc. 82 (1999) 269–280.
[5] G. Bate, J. Magn. Magn. Mater. 100 (1999) 413–424.
[6] J.M. Xue, Z.H. Zhou, J. Wang, Mater. Chem. Phys. 75 (2002) 81–85.
[7] C. Cannas, D. Gatteschi, A. Musinu, G. Piccalunga, C. Sangregorio, J. Phys. Chem. B 102 (1998) 7721–7726.
[8] R.M. Cornel, U. Schwertmann, The iron oxides, in: Structure, Properties, Reactions, Occurrence and Uses, VCH, Weinheim, 1996.
[9] R. Zboril, M. Mashlan, D. Petridis, Chem. Mater. 14 (2002) 969–982.
[10] E. Tronc, C. Chanéac, J.P. Jolivet, J. Solid State Chem. 139 (1998) 93–104.
[11] P. Ayyuh, M. Multani, M. Barma, V.R. Polkar, R. Vijayaravan, J. Phys. C: Solid State Phys. 21 (1998) 2229–2245.
[12] F. Bentivegna, J. Ferre, M. Nyvlt, J.P. Jamet, D. Imhoff, M. Canva, A. Brun, P. Veillet, S. Visnovsky, F. Chaput, J.P. Boilot, J. Appl. Phys. 83 (1998) 7776–7787.
[13] M. Popovici, M. Gich, D. Niznansky, A. Roig, C. Savii, L. Casas, E. Molins, K. Zaveta, C. Enache, J. Sort, S. Brion, G. Chouteau, J. Nogués, Chem. Mater. 16 (2004) 5542–5548.
[14] I.K. Battisha, H.H. Afify, I.M. Hamada, J. Magn. Magn. Mater. 292 (2005) 440–446.
[15] Y.S. Kang, S. Risbud, J.F. Rabolt, P. Stroeve, Chem. Mater. 8 (1996) 2209–2211.
[16] B.D. Cullity, Elements of X-ray Diffraction, Addison-Wesley, Canada, 1978.
[17] P.C. Morais, E.C.D. Lima, D. Rabelo, A.C. Reis, F. Pelegrini, IEEE Trans. Magn. 36 (2000) 3038–3040.
[18] T. Belin, T. Guigue-Millot, T. Caillot, J. Solid State Chem. 163 (2002) 459–465.
[19] R.C. Pedroza, S.W. Silva, M.A. Soler, P.P.C. Sartoratto, D.R. Resende, P.C. Morais, J. Magn. Magn. Mater. 289 (2005) 139–141.
[20] M.H. Sousa, J.C. Rubim, P.G. Sobrinho, F.A. Tourinho, J. Magn. Magn. Mater. 225 (2001) 67–72.
[21] P. Yuan, H.P. He, D.Q. Wu, D.Q. Wang, L.J. Chen, Spectrochim. Acta Part A 60 (2004) 2941–2945.
[22] V. Vendange, D.J. Jones, Ph. Colomban, J. Phys. Chem. Solids 57 (1996) 1907–1918.
[23] C. Chanéac, E. Tronc, J.P. Jolivet, Nanostruct. Mater. 6 (1995) 715–718.
[24] G. Schimanke, M. Martin, Solid State Ionics 136–137 (2000) 1235–1240.